JACS
JOURNAL OF THE AMERICAN CHEMICAL SOCIETY
Article
pubs.acs.org/JACS

Interplay between 1,3-Butadien-1,4-diyl and 2-Buten-1,4-dicarbene Derivatives: The Quest for Nucleophilic Carbenes

Gebhard Haberhauer*,† and Rolf Gleiter*,‡

†Institut für Organische Chemie, Universität Duisburg-Essen, Universitätsstrasse 7, D-45117 Essen, Germany
‡Organisch-Chemisches Institut, Universität Heidelberg, Im Neuenheimer Feld 270, D-69120 Heidelberg, Germany

Supporting Information

ABSTRACT: By means of high level quantum chemical calculations, the influence of electron-donating heteroatomic groups (O, NH) was investigated on the 1,6-transannular ring closure of 1,6-cyclodecadiyne (**8a**). In the case of **8a**, the bicyclo[4.4.0]deca-1,6-dien-2,7-diyl biradical **12** is generated. It was found that oxygen centers or NH groups next to the triple bond reduce the activation energy of the ring closure considerably. For the intermediate, a 2-buten-1,4-dicarbene derivative is predicted. The extension of the model calculations to two hydroxyl- or aminoacetylenes predicts the formation of the corresponding 1,3-butadien-1,4-diyl intermediates or the 2-buten-1,4-dicarbene derivatives, a member of the nucleophilic carbene family. Moreover, the calculations predict that two separated dimethoxyacetylenes are more than 7 kcal/mol less stable than the corresponding biradical and dicarbene, respectively. Possible reactions of the dicarbenes with transition metal compounds are discussed.

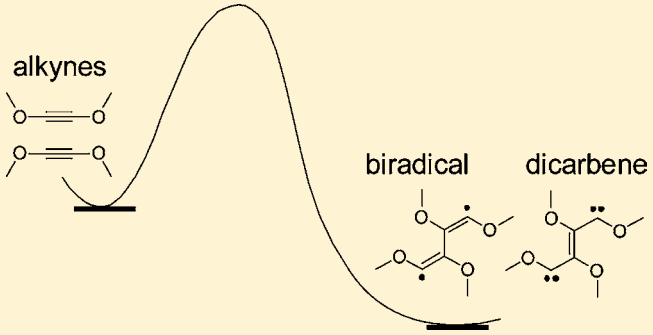

INTRODUCTION

Two triple bonds, fixed parallel in close proximity, react with each other via a *trans*-1,3-butadien-1,4-diyl intermediate. This was first reported when Mitchell and Sondheimer[1] tried to generate dinaphth-1,6-didehydro[10]annulene (**2**) from the precursor **1** (Scheme 1).

Scheme 1. Generation of Zethrene (4) via 2 and 3 from 1

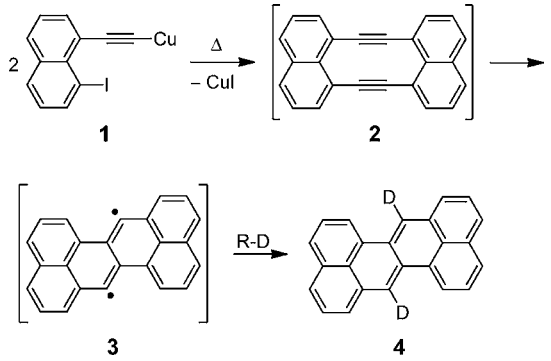

When **1** was treated in boiling pyridine, only zethrene (**4**) could be isolated in 22% yield. These results were confirmed by Staab et al.[2] A related reaction was found when Myers and Finney prepared 1,6-didehydro[10]annulene (**5**)[3] (Scheme 2). This species could only be studied at temperatures below −90 °C. At higher temperatures, it cyclized to naphthalene (**7**) via the 1,5-dehydronaphthalene (**6**) intermediate. In line with these observations were experiments with 1,6-cyclodecadiyne (**8a**) and some of its derivatives.[4] When *N*,*N*′-diisopropyl-1,6-diazacyclodeca-3,8-diyne (**8b**) was heated with hydrocarbons,[4a] or the parent system **8a** was treated with CCl_4, $(SCN)_2$, or BrCN,[4b] the products were rationalized by assuming bicyclo[4.4.0]deca-1,6-dien-2,7-diyl (**12**) as intermediate (see Schemes 3 and 4).[4,5]

Scheme 2. Thermal Rearrangement of 1,6-Didehydro[10]annulene (5) to 1,5-Dehydronaphthalene (6)

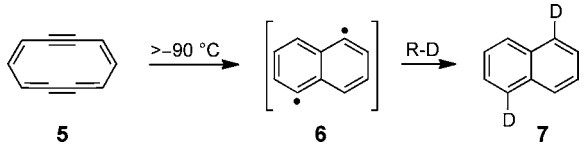

The energetic parameters of **12** were measured by using the trapping rate of **8a** with NO and O_2 in the gas phase and in supercritical CO_2 in the temperature range 160−240 °C.[5a]

These studies yielded the activation enthalpy of 28.6 ± 0.4 kcal/mol for the reaction of **8a** to **12** as shown in Scheme 4. For the biradical **12**, a heat of formation of 116.2 kcal/mol was measured.[5a] By using CASPT2[g1]/6-31G* calculations, the activation enthalpy was calculated to be 21.4 kcal/mol.[5b] These latter investigations suggest also that the 1,6-ring closure is favored by 7 kcal/mol with respect to the 1,5-ring closure to **14**

Received: March 2, 2013
Published: April 28, 2013

   dx.doi.org/10.1021/ja4020937 | J. Am. Chem. Soc. 2013, 135, 8022−8030

Scheme 3. Reactions of 8a with Halogens or Pseudohalides to 9 or of 8b with Hydrocarbons to 10

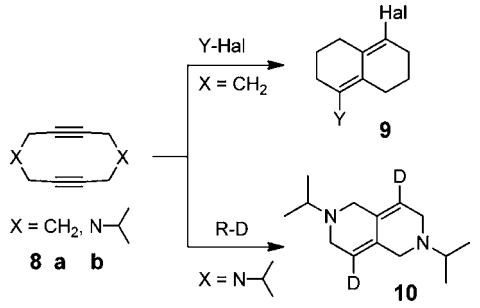

Scheme 4. Generation of 12 and 14 from 8a via 1,6- or 1,5-Ring Closure

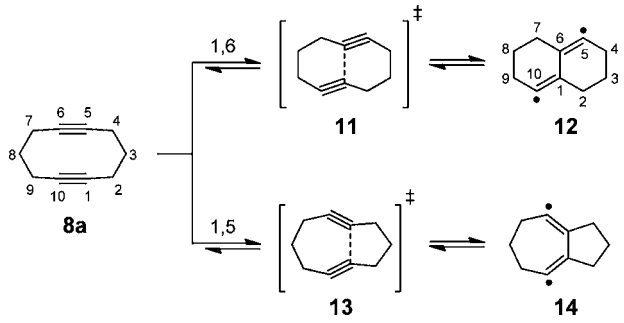

Scheme 5. Heterocyclic Model Systems 15, 18, 21 and Their Expected Products 17, 20, 23

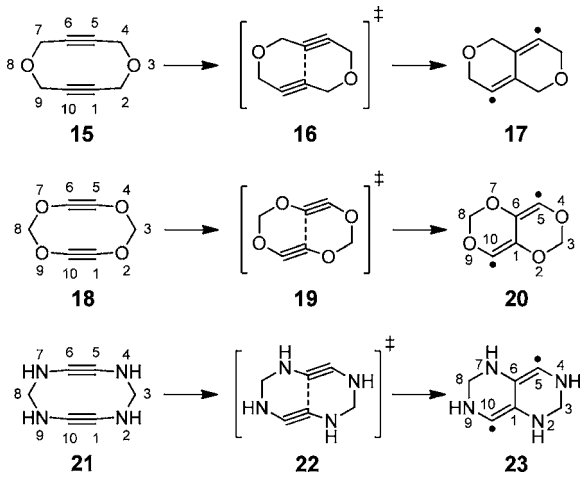

(see Scheme 4). Our theoretical studies on the transannular ring closure of **8a** to **12** show that the $2p_\sigma$ orbitals at centers 5 and 10 of **12** interact rather strongly through-bond, and thus in the biradical **12** the occupation number of the HOMO ($18a_u$) is larger than the LUMO ($19a_g$), and hence the triplet state ^3A_u is predicted above the singlet state ^1A_g.[5b]

To find out if the transannular ring closure of two triple bonds in a 10-membered ring system can be influenced by substituent effects, we have carried out model calculations on various cyclic congeners as shown in Scheme 5. Later, we extended our investigations on the dimerization of simple substituted alkynes.

METHODOLOGY AND BENCHMARK CALCULATIONS

All calculations were performed by using the program package Gaussian 09[6] and MOLPRPO.[7] From our earlier calculations of the potential energy of the reaction profile of **8a** to **12** (Scheme 4),[5b] we experienced that dynamic correlation effects have to be included to describe the biradical **12** properly. In this work, we used the double hybrid method B2PLYPD by Grimme[8] and coupled cluster (CCSD-(T)) calculations[9] and compared them to results derived by the MP4SDQ,[10] MP2,[11] CASSCF,[12] and CASPT2[13] levels of theory.

The geometrical parameters of the stationary points were optimized by means of B2PLYPD-full (for all) and (12,10)CASSCF (for **8a**, **11**, **12**, and **18**−**20**) calculations. As basis sets the 6-31+G**[14] and the aug-cc-pVDZ[15] have been used. We further assumed that C_i symmetry is maintained during the reaction. For the alkynes **27** and **31** C_s symmetry, for alkyne **24** C_{3v} symmetry, for alkyne **35** no symmetry restriction, and for all other stationary points C_i symmetry was applied. The reactions of **18** to **20** and of **27** to **29** have also been calculated without symmetry restriction. The obtained results did not differ from those obtained within C_i symmetry. Frequency calculations were carried out at each of the structures to verify the nature of the stationary point. It turned out that the alkynes, diynes, bicyclic biradicals, and dicarbenes have no imaginary frequency, whereas the transition states have exactly one. The energies of the stationary points were calculated using B2PLYPD-full/aug-cc-pVDZ (for **8a**, **11**, and **12**), (12,10)CASSCF (for **8a**, **11**, **12**, and **18**−**20**), (12,10)CASPT2 (for **8a**, **11**, **12**, and **18**−**20**), MP4SDQ-FC (for **8a**, **11**, and **12**), MP2-FC (for **8a**, **11**, and **12**), and CCSD(T)-FC. The 6-311++G** and 6-311++G(3d,2p) basis sets[16] were employed. To obtain the potential energy curves for the cyclization, the distance C1···C6 was fixed at a specific value, and all other geometric variables were optimized using B2PLYPD-full within the C_i point group. A similar procedure was used to study the C−C bond formation of two alkyne units. Here, the reaction profiles of the dimerization were obtained by calculating the energies of about 15 points of the surface by varying the C1−C1′ distance R between 4.00 and 1.40 Å. All other geometrical parameters of the dimers were optimized within C_i symmetry on the level of the B2PLYPD-full theory.

As the experimental data for the cyclization of **8a** to **12** are known, we used this reaction for benchmark calculations. The results for different methods (all of them but the CASSCF method include the dynamic correlation effects) and different basis sets are compared in Table 1 to those of the experiment. It is found that the first three approaches ((a)−(c)) reproduce the energies of **11** and **12** with respect to **8a** quite well. The best agreement is found for method (c). The comparison also shows that the results derived by the Møller−

Table 1. Comparison between the Results of the Methods of Calculations ((a)−(g)) for the Distance R = C1−C6 and the Difference ΔE (kcal/mol) of the Activation Energy between 8a and 11 and 12, Respectively

	R [Å][a]	ΔE (exp)[5a]	ΔE^a	ΔE^b	ΔE^c	ΔE^d	ΔE^e	ΔE^f	ΔE^g
8a	3.247	0.0	0.0	0.0	0.0	0.0	0.0	0.0	0.0
11	1.811	28.9	27.9	26.6	28.1	37.7	22.1	43.8	19.0
12	1.561	24.6	26.1	24.6	24.7	41.5	14.7	42.2	14.4

[a]B2PLYPD/6-31+G**. [b]B2PLYPD/aug-cc-pVDZ//B2PLYPD/6-31+G**. [c]CCSD(T)/6-311++G**//B2PLYPD/6-31+G**. [d]MP4SDQ/6-311++G**//B2PLYPD/6-31+G**. [e]MP2/6-311++G**//B2PLYPD/6-31+G**. [f](12,10)CASSCF/6-311++G**//(12,10)CASSCF/6-31+G**. [g]CASPT2/6-311++G**//(12,10)CASSF/6-31+G**.

dx.doi.org/10.1021/ja4020937 | J. Am. Chem. Soc. 2013, 135, 8022−8030

Plesset approach (d,e), the CASSCF (f), and the CASPT2 (g) methods differ considerably from experiment.

This comparison is also illustrated in Figure 1 where the energy profiles derived for the reaction of **8a** to **12** are plotted as a function of

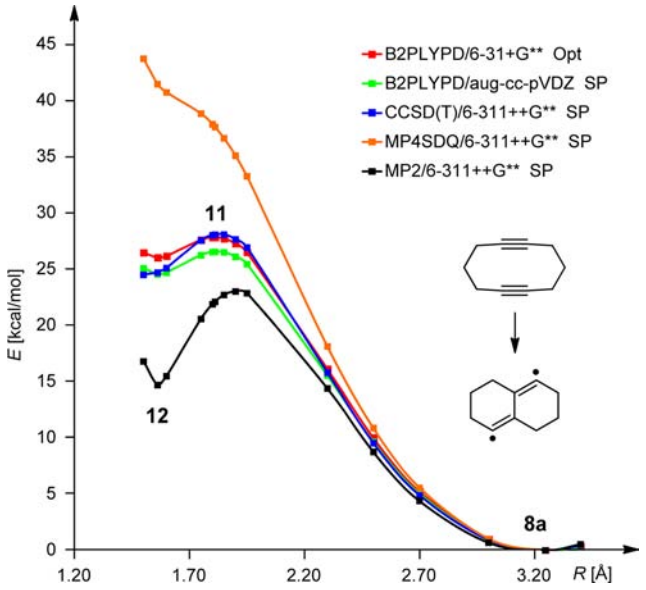

Figure 1. Energy profile of **8a** to **12** as derived by various levels of theory. The energies are given as a function of *R*, the distance between centers 1 and 6. Abbreviations used: Opt for optimization and SP for single point calculation.

the C1···C6 distance *R*. We decide to use for further investigations the B2PLYPD level of theory for the optimization of the geometrical parameters. The energies of the stationary points were calculated in a further step by the CCSD(T) level of theory. This choice is based on our above-mentioned experience of calculations of biradicals such as **12** and related ones from Bergman cyclizations.[17] A single reference method seems in our case reasonable due to the aforementioned strong difference of the occupation numbers of the radical centers.

RESULTS AND DISCUSSION

a. Cyclic Diynes. To study the influence of free electron pairs of heteroatoms on the intramolecular 1,6-ring closure, we calculated the reaction profile of **15**, **18**, and **21**, the congeners of **8a**. The potential energy curves (Figure 2) were derived by calculating about 15 points on the surface by means of the B2PLYPD/6-31+G** procedure. The relative energies of the transition states (**16**, **19**, **22**) and of the bicyclic products (**17**, **20**, **23**) were also derived by means of single point calculations using the CCSD(T)/6-311++G**//B2PLYPD/6-31+G** procedure as given in Table 2. This table contains also the singlet−triplet energy differences (Δ*E*(S−T)) using the same level of theory.

The calculations reveal a lowering of the barriers from **11** to **16** by about 7 kcal/mol, from **11** to **19** by 20 kcal/mol, and from **11** to **22** by 15 kcal/mol based on the CCSD(T) calculations (Table 2). The most striking result is the strong stabilization of the bicyclic products **20** and **23** (cf., Table 2 and Figure 2). To rationalize these findings, we consider in Figure 3 at the left side a qualitative correlation diagram between the frontier orbitals of **8a** and **12**, assuming C_i symmetry. During the 1,6-ring closure, the occupied out-of-plane π orbital $a_g(\pi_o)$ and the occupied in-plane π orbital $a_u(\pi_i)$ of **8a** will be destabilized, whereas the unoccupied in-plane π orbital $a_g(\pi_i^*)$ will be stabilized. This brings the $a_u(\sigma)$ (HOMO) and $a_g(\sigma)$

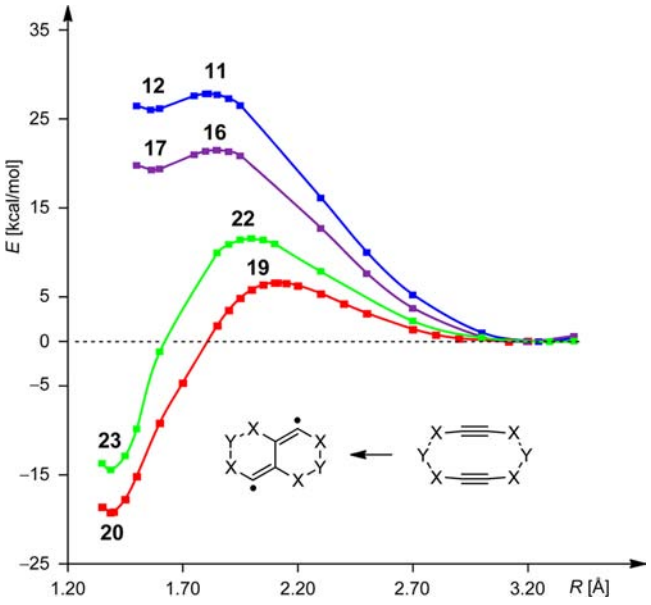

Figure 2. Energy profiles for the transannular ring closure of **8a** to **12** (blue; X = Y = CH_2), **15** to **17** (purple; X = CH_2, Y = O), **18** to **20** (red; X = O, Y = CH_2), and **21** to **23** (green; X = NH, Y = CH_2) as a function of the C1···C6 distance *R* using B2PLYPD/6-31+G**.

Table 2. Energy Differences (Δ*E*, kcal/mol) between the Various Starting Materials 8a, 15, 18, 21 and Their Corresponding Transition States (11, 16, 19, 22) and Bicyclic Products (12, 17, 20, 23) as a Function of *R*, the C1···C6 Distance[a]

	R [Å][b]	Δ*E*[b]	Δ*E*[c]	Δ*E*(S−T)[d]
8a	3.247	0.0	0.0	
11	1.811	27.9	28.1	
12	1.561	26.1	24.7	9.4
15	3.195	0.0	0.0	
16	1.846	21.5	21.3	
17	1.565	19.3	17.8	12.2
18	3.116	0.0	0.0	
19	2.112	6.6	7.5	
20	1.386	−19.2	−18.8	18.7
21	3.294	0.0	0.0	
22	1.996	11.6	12.0	
23	1.388	−14.4	−17.2	33.8

[a]Also given are the singlet−triplet splitting (Δ*E*(S−T)) in the products and the calculation procedures. [b]B2PLYPD/6-31+G**. [c]CCSD(T)/6-311++G**//B2PLYPD/6-31+G**. [d]Singlet−triplet energy difference with CCSD(T)/6-311++G**//B2PLYPD/6-31+G**.

(LUMO) orbitals relatively close together. According to our calculations, the energy difference between HOMO and LUMO is quite sizable; therefore, mainly the HOMO is populated (cf., Table 3, below). Please note that due to through-bond interaction[18] in **12** the antibonding linear combination ($a_u(\sigma)$) of the nonbonding orbitals at C5 and C10 is lower in energy than the bonding linear combination ($a_g(\sigma)$) and thus represents the HOMO in **12**.

In the case of **18** (right side of Figure 3), the $a_g(\pi_o)$ orbital is considerably destabilized due to a strong antibonding interaction between the p_π orbitals at the sp carbons and oxygen. In the case of a 1,6-ring closure, the $a_g(\pi_i^*)$ will be stabilized and the $a_g(\pi_o)$ orbital will be destabilized. As a result

dx.doi.org/10.1021/ja4020937 | J. Am. Chem. Soc. 2013, 135, 8022−8030

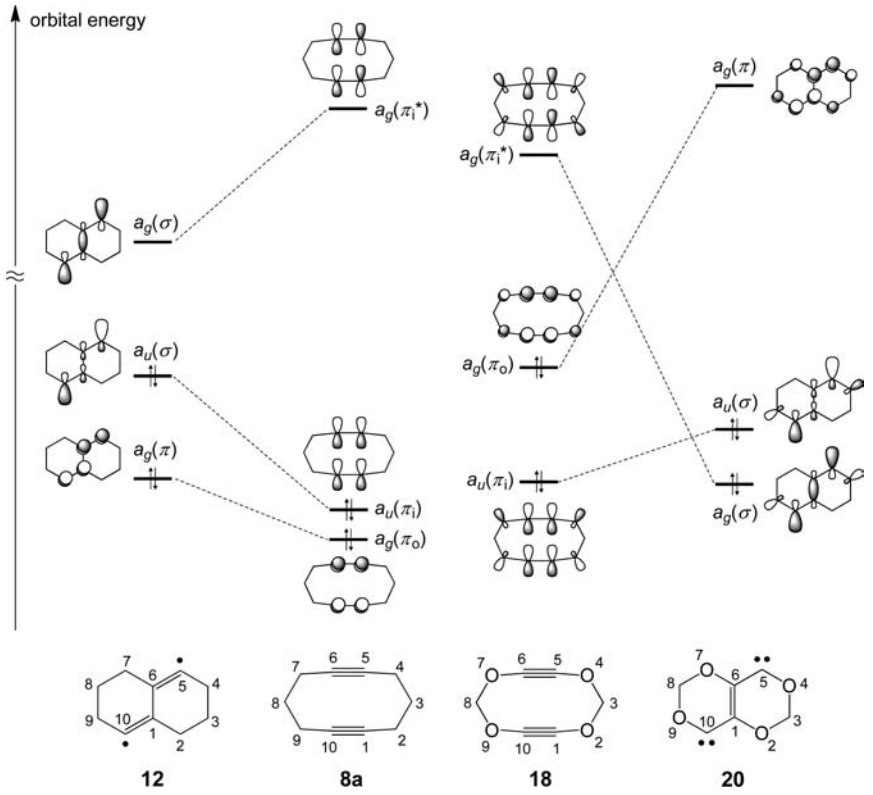

Figure 3. Correlation of frontier orbitals for the ring closure of **8a** to **12** and **18** to **20**, assuming C_i symmetry for starting materials and products. For comparison we used the same numbering for all molecules.

Table 3. Selected NBO Results Derived for 12, 20, and 23 by Means of HF/6-311++G//B2PLYPD/6-31+G** Calculations[a]**

compound	bonds	occupation number
12	π (C1−C10; C5−C6)	1.92
	n_1 (C5,C10)[b]	1.73
	n_2 (C5,C10)[c]	0.34
20	π (O4−C5; O9−C10)	1.97
	π (C1−C6)	1.82
	n (C5; C10)	1.91
23	π (N4−C5; N9−C10)	1.97
	π (C1−C6)	1.83
	n (C5; C10)	1.91

[a]For numbering of the atoms in **12**, **20**, and **23**, see Schemes 4 and 5. [b]n_1 antibonding linear combination ($a_u(\sigma)$) of the nonbonding orbitals at C5 and C10. [c]n_2 bonding linear combination ($a_g(\sigma)$) of the nonbonding orbitals at C5 and C10.

of this crossing, two electrons from the $a_g(\pi)$ orbital are formally transferred to the $a_g(\sigma)$ orbital. Thus, in **20** both orbitals with large coefficients at C5 and C10 are occupied. In the case of the ring closure of **8a** to **12**, such a crossing does not occur. Therefore, only one orbital ($a_u(\sigma)$) with large coefficients at C5 and C10 is (mainly) occupied. The correlation diagram in Figure 3 predicts a biradical for **12** and a dicarbene for **20**. For the ring closure of **21** to **23**, our calculations predict also a dicarbene, centered at positions 5 and 10.

The electronic structures for **12**, **20**, and **23** as derived from Figure 3 are corroborated by an NBO[19] analysis based on a HF calculation. The resulting occupation numbers are compiled in Table 3 for **12**, **20**, and **23**. We notice for **12** strong π bonds for C1−C10 and C5−C6 (1.92 electrons). The antibonding linear combination of the radical centers (n_1), which is represented by the $a_u(\sigma)$ orbital, is occupied by 1.73 electrons, whereas the bonding linear combination (n_2) of the radical centers ($a_g(\sigma)$) is occupied by 0.34 electrons. These latter values are in agreement with a small singlet−triplet splitting of 9.4 kcal/mol for **12** as shown in Table 2. For **20**, we find for the O4−C5, O9−C10 bonds a strong π character of 1.97 electrons, stronger than for the C1−C6 bond (1.82 electrons). The nonbonding carbene orbitals (n) at C5 and C10 are occupied by 1.91 electrons. In agreement with these results is a strong singlet−triplet splitting of 18.7 kcal/mol for **20**. For the reaction of **21** to **23**, one obtains a closely related correlation diagram as for the reaction of **18** to **20**. The high lying $a_g(\pi_o)$ orbital is strongly destabilized, and the low lying $a_g(\pi_i^*)$ orbital is stabilized. As a consequence, two high lying σ orbitals result (a_u, a_g) with large coefficients at C5 and C10. Because of this orbital crossing, the NBO analysis (Table 3) shows very similar occupation numbers in the case of **23** as for **20**. The results listed in Table 3 are "translated" into a valence bond representation of **12**, **20**, and **23** in Figure 4. The predicted properties for **12** suggest a singlet biradical, whereas for **20** and **23** one expects a nucleophilic dicarbene with a singlet ground state.

If we consider once again the correlation diagram for the cyclization of **18** to **20** (Figure 3), one can see that there is a crossing between a filled and empty orbital along the reaction coordinate. During this crossing, two electrons from the $a_g(\pi)$ orbital are formally transferred to the $a_g(\sigma)$ orbital. As the used methods (B2PLYPD and CCSD(T)) are based on a single reference configuration, there is discontinuous change of this reference wave function along the reaction coordinate. In the

dx.doi.org/10.1021/ja4020937 | J. Am. Chem. Soc. 2013, 135, 8022−8030

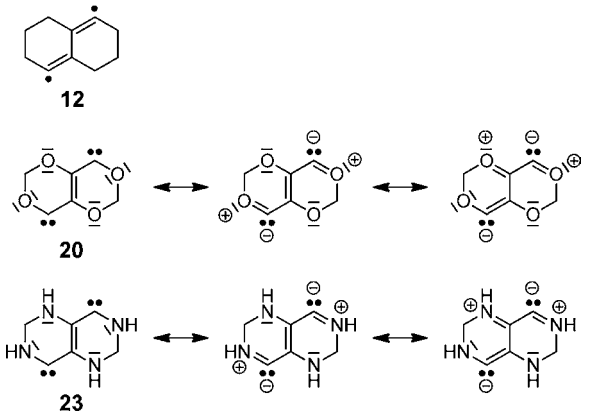

Figure 4. Valence bond formulations of **12**, **20**, and **23**.

range of this change, neither B2PLYPD nor CCSD(T) is able to describe the molecule properly. To check if the change of this reference wave function is far from the transition state, (12,10)CASSCF/6-311++G** and (12,10)CASPT2/6-311++G** single point (SP) calculations were performed. The geometric parameters of the points along the reaction coordinate were optimized (Opt) using (12/10)CASSCF/6-31+G** and B2PLYPD/6-31+G**, respectively (see Figure 5). A comparison of the energy profiles for the cyclization of **18** to **20** shows that with CASSCF and CASPT2 methods two minima for **20** are found. The one with a C1−C6 distance of 1.50 Å represents the biradical **20**(br), whereas the minimum at a C1−C6 distance of 1.36 Å is the dicarbene **20**(dc). Interestingly, the CASPT2 energies for the biradical **20**(br) and dicarbene **20**(dc) (−21.8 and −18.6 kcal/mol) are lower if their geometric parameters are optimized by B2PLYPD/6-31+G** as compared to the values obtained by (12,10)-CASPT2/6-311++G**//(12/10)CASSCF/6-31+G** (−20.5 and −14.0 kcal/mol). The energy for the dicarbene **20**(dc) (−18.6 kcal/mol) calculated by means of CASPT2//B2PLYPD agrees very well with the value obtained by CCSD(T)// B2PLYPD (−18.8 kcal/mol). Independent of the used method for the optimization of the geometric parameters, the CASPT2 energy of the biradical **20**(br) is lower than the value for the dicarbene **20**(dc). However, this result should be handled with care as the CASPT2 approximation is prone to overestimate the stabilization of biradical states.[5b] For example, the value calculated by means of CASPT2 for **12** is lower by about 10 kcal/mol than the experimental one observed (Table 1). Bearing this in mind, one can doubt if the biradical **20**(br) represents a minimum on the reaction profile at all.

An analysis of the CASSCF wave function should allow the determination of the biradical character of a stationary point. As a measure of the biradical character of the transition state **19** and the biradical **20**(br), the occupation numbers of the frontier orbitals $a_u(\sigma)$ and $a_g(\sigma)$ can be used. In a perfect biradical, both frontier orbitals would be equally populated. A comparison shows that the biradical character increases on going from **18** via **19** to **20**(br) (Table 4 and Supporting Information). For **20**(br), the calculated values for the occupation numbers for $a_u(\sigma)$ and $a_g(\sigma)$ are close to that found for the biradical **12**. Thus, **12** and **20**(br) are still far from being "perfect", which is due to a strong through-bond interaction between the orbitals of the radical centers. In the case of the dicarbene **20**(dc), the orbitals $a_u(\sigma)$ and $a_g(\sigma)$ are almost completely occupied, whereas the orbital $a_g(\pi)$ exhibits a rather small occupation number. Hence, the description of the dicarbene **20**(dc) using a single reference method such as CCSD(T) and B2PLYPD is justified. The above-mentioned change in the configuration of the reference wave function occurs in the area between 1.50 and 1.40 Å.

b. Two Alkynes. The unexpected behavior of **20** and **23** encouraged us to investigate the C−C bond formation of two alkynes substituted by one or two donor groups. The models used in our investigations are shown in Scheme 6. To obtain the reaction profile of the products of a C1−C1′ or C2−C2′ dimerization, we calculated the energies of about 15 points of the surface by varying the C1−C1′ or C2−C2′ distance *R* between 4.00 and 1.40 Å. All other geometrical parameters of

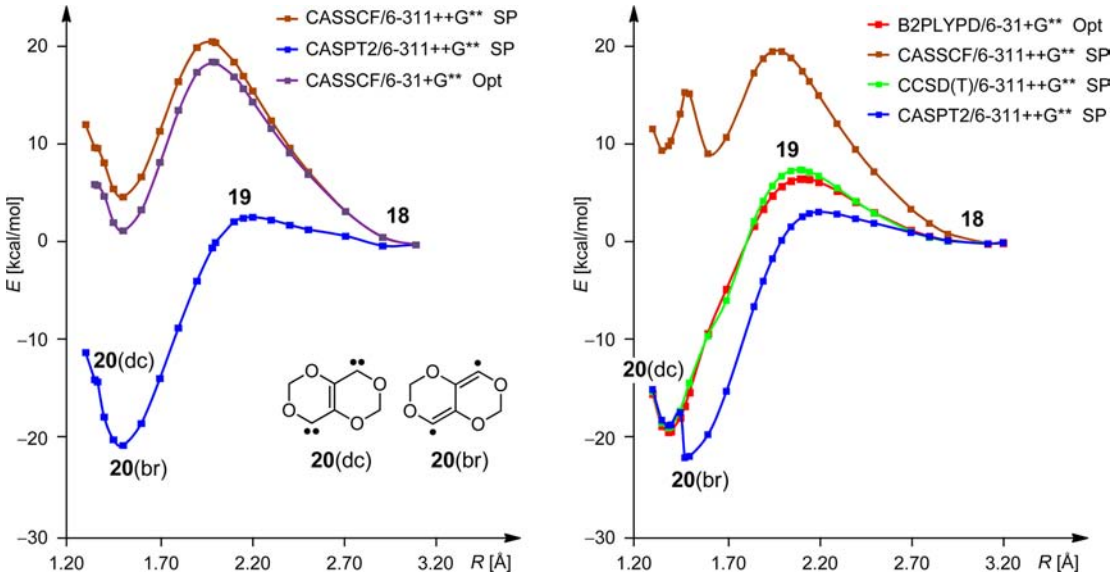

Figure 5. Energy profile of **18** to **20** as derived by various levels of theory. The energies are given as a function of *R*, the distance between centers 1 and 6. The geometric parameters were optimized using (12/10)CASSCF/6-31+G** (left) and B2PLYPD/6-31+G** (right). Abbreviations used: Opt for optimization, SP for single point calculation, br for biradical, and dc for dicarbene.

dx.doi.org/10.1021/ja4020937 | *J. Am. Chem. Soc.* 2013, 135, 8022−8030

Table 4. Occupation Numbers of Selected Natural Orbitals of 8a, 11, 12, and 18−20[a]

orbitals	8a[b]	11[b]	12[b]	18[b]	19[b]	20(br)[b]	20(dc)[c]
$a_g(\pi_i^*)/a_g(\sigma)$	0.062	0.336	0.556	0.065	0.237	0.648	1.946
$a_u(\pi_i)/a_u(\sigma)$	1.933	1.670	1.450	1.930	1.770	1.360	1.906
$a_g(\pi_o)/a_g(\pi)$	1.941	1.911	1.881	1.941	1.923	1.863	0.105

[a]The results are taken from (12,10)CASSCF/6-311++G** calculations. Some selected natural orbitals are also depicted in the Supporting Information. [b]Geometry parameters were optimized using (12,10)CASSCF/6-31+G**. [c]Geometry parameters were optimized using B2PLYPD/6-31+G**.

Scheme 6. Possible Dimerization Products from Two Alkynes 24·24, 27·27, 31·31, and 35·35

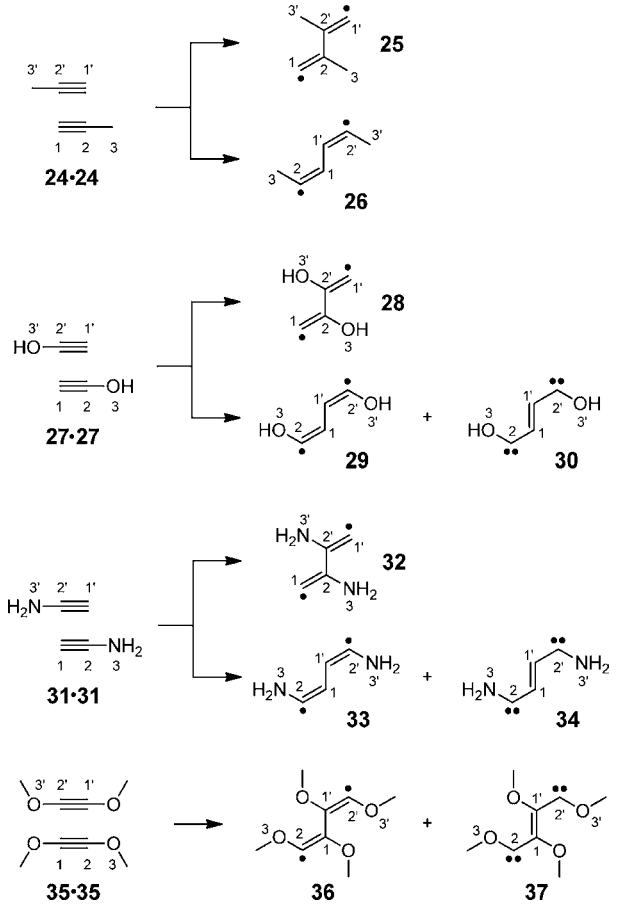

the dimers were optimized on the level of the B2PLYPD theory. To determine the energies of the transition states and the final products, we also used the CCSD(T) level of theory (see Table 5). The energy values presented in Table 5 are throughout higher for the C2−C2′ bond formation as compared to the C1−C1′ bond closure; therefore, we used in Figure 6, where we compare the energy profiles for the C−C bond formation, only the results for the C1−C1′ bond closure. A comparison between the potential energy curves of the cyclic species **8a**, **18**, **21** (cf., Figure 2) with those of **24**, **27**, **31**, and **35** (Figure 6) reveals a similar behavior: the pure hydrocarbons (**8a** and **24**) show the highest activation energy, and the biradicals **12** and **26** are about 25 kcal/mol less stable than the starting materials. The activation energy is lowered when heteroatoms with free electron pairs are attached directly to the triple bonds, **18** and **21** for cyclic species, and **27**, **31**, and **35** for noncyclic model systems. In the case of the oxygen-containing compound, the biradical **29** is of stability similar to that of the corresponding dicarbene **30**. The nitrogen-containing dicarbene **34** is much more stable than the corresponding biradical **33**.

Table 5. Energy Differences (ΔE in kcal/mol) between the Various Starting Materials (24, 27, 31, and 35), Transition States, and Corresponding Products[a]

compound	R [Å][b]	ΔE^b	ΔE^c
24	–[d]	0.0	0.0
24·24#	1.82	26.7	31.4
26	1.54	23.6	27.0
25	1.56	29.9	30.6
27	–[d]	0.0	0.0
27·27#	1.97	18.0	21.5
29	1.47	4.0	5.6
30	1.38	4.1	8.0
28	1.50	8.7	8.0
31	–[d]	0.0	0.0
31·31#	1.95	19.1	23.5
33	1.48	7.0	11.5
34	1.38	−8.7	−3.3
32	1.54	21.0	20.9
35	–[d]	0.0	0.0
35·35#	2.07[e]	6.3[f]	13.3[f]
36	1.47[e]	−16.5[f]	−7.7[f]
37	1.40[e]	−14.2[f]	−7.9[f]

[a]The distances R of C1−C1′ and C2−C2′ are also given. [b]B2PLYPD/aug-cc-pVDZ. [c]CCSD(T)/6-311++G(3d,2p)//B2PLYPD/aug-cc-pVDZ. [d]The monomeric alkynes were used as references. [e]B2PLYPD/6-31+G**. [f]CCSD(T)/6-311++G**//B2PLYPD/6-31+G**.

For two dimethoxyacetylenes (**35·35**), our calculations predict that the biradical **36** is of stability similar to that of the corresponding dicarbene **37**. Furthermore, the activation barrier for the dimerization of **35** is much lower than that for **27** and **31**. Yet the most striking aspect is that the calculations predict that two separated alkynes **35** are more than 7 kcal/mol less stable than the corresponding biradical **36** and dicarbene **37**, respectively.

To rationalize the data obtained for **24**, **27**, **31**, and **35**, we have compared in Figure 7 the frontier orbitals of two propynes (**24·24**) producing hexa-2,4-dien-2,5-diyl (**26**) (left side Figure 7) with two hydroxyacetylenes (**27·27**) giving rise to the dicarbene **30** (right side of Figure 7). Similar to Figure 3, the heteroatoms in **27** cause an orbital crossing by destabilizing the occupied π (b_g) linear combination and stabilizing the σ (a_g) orbital of **27·27** during the C1−C1′ bond formation. Finally, in **30** both carbon "lone" pairs b_u and a_g are occupied, whereas in **26** only b_u was occupied. This latter situation resembles that experienced for the ring closure of **18** to **20** very much as shown in Figure 3.

For **26**, **29**, **30**, **33**, **34**, **36**, and **37**, NBO analyses based on HF calculations confirm the electronic structures of the different dimerization products (see Table 6). For the biradicals

dx.doi.org/10.1021/ja4020937 | J. Am. Chem. Soc. 2013, 135, 8022−8030

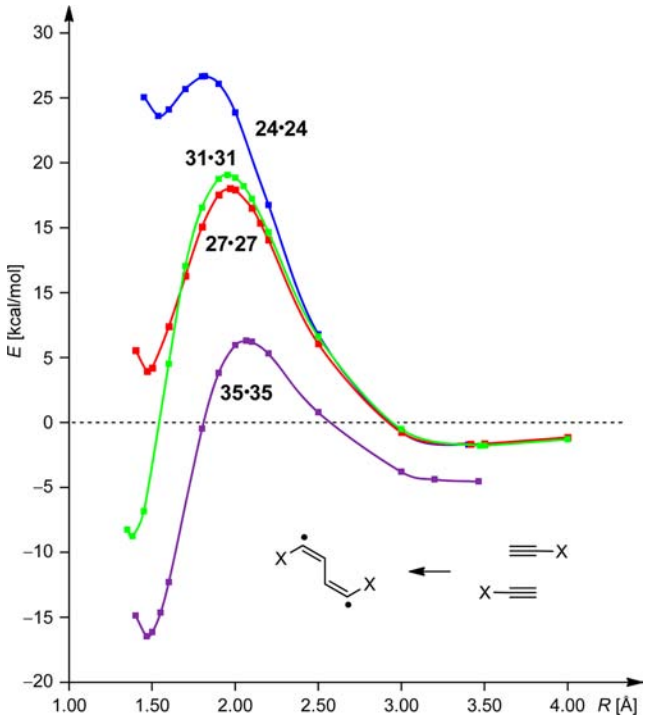

Figure 6. Energy profiles for the C1−C1′ bond formation of **24·24** (blue), **27·27** (red), **31·31** (green), and **35·35** (violet) using B2PLYPD/aug-cc-pVDZ (for **24·24**, **27·27**, and **31·31**) and B2PLYPD/6-31+G** (for **35·35**).

26, **29**, **33**, and **36**, two strong π bonds for C1−C2 and C1′−C2′ are found. The antibonding linear combinations of the radical centers are occupied by 1.72−1.76 electrons. In the bonding linear combination of the radical centers of **26**, 0.30 electrons are found. Because of the electron-donating effect of the nitrogen and oxygen, the bonding linear combinations of the radical centers in **29**, **33**, and **36** are occupied by 0.37−0.46 electrons, which is a little bit higher than the value found for the hydrocarbon **26**.

For the dicarbenes **30**, **34**, and **37**, we find strong π bonds between C1−C1′, which are occupied by 1.81−1.88 electrons. The nonbonding carbene orbitals n_{sp} at C2 and C2′ have occupation numbers of values of 1.86−1.93 electrons. In the case of **34** and **37**, strong π bonds are found between C2−N3 (C2−O3) and C2′−N3′ (C2′−O3′) showing an occupation number of 1.97 electrons. For dicarbene **30**, we find no π bond between C2−O3, but two nonbonding orbitals at the oxygen O2 (not given in Table 6) and a p orbital at the carbene center, which is occupied by 0.28 electrons.

The molecular structures of the dicarbenes differ besides the lengths of the C1−C1′ bond distinctly from that found for the corresponding biradicals (see the Supporting Information). In the biradical **29**, the n_p orbitals of the oxygen atoms are in the same plane as the orbitals of the radical centers. On the contrary, in the dicarbene **30**, the n_p orbitals of the oxygen atoms are perpendicular to the n_{sp} carbene orbitals. This orientation leads to a stabilizing interaction with the empty p orbital of the carbene centers and avoids a 4-electron repulsion with the n_{sp} carbene orbitals. Similar behaviors are found for the biradical **33** and **36** as well as the dicarbenes **34** and **37**.

CONCLUSION, POSSIBLE APPLICATIONS, AND EXPERIMENTAL RESULTS

In summary, we were able to show that the transannular ring closure of cyclic decadiynes and the dimerization of alkynes are strongly affected by electron-donating heteroatomic groups (O, NH). It was found that oxygen centers and NH groups next to the triple bonds reduce the activation barrier and stabilize the formed 1,4-biradical. These effects are stronger for the oxygen-containing compounds. Beside the 1,4-biradicals, 1,4-dicarbenes

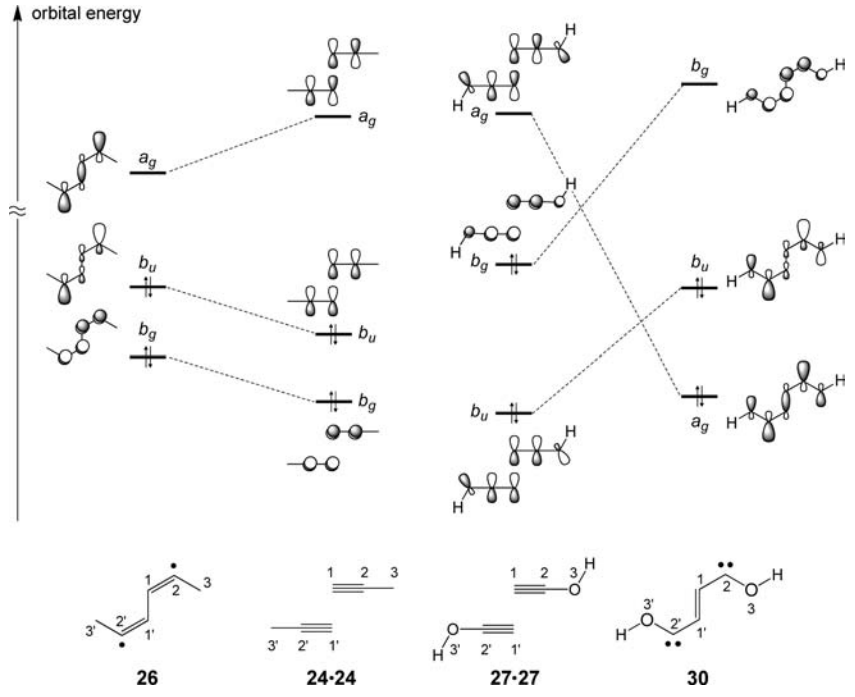

Figure 7. Correlation between the frontier orbitals for the 1,1′ interaction of two propynes (left) and two hydroxyacetylenes (right), assuming C_{2h} symmetry for starting materials and products. For comparison we used the same numbering for all molecules.

dx.doi.org/10.1021/ja4020937 | J. Am. Chem. Soc. 2013, 135, 8022−8030

Table 6. Selected NBO Results Derived for 26, 29, 30, 33, 34, 36, and 37 by Means of HF Calculations

compound	bonds/occupation number		
26[a]	π (C1−C2)/1.95	n_1 (C2,C2′)[c]/1.72	n_2 (C2,C2′)[d]/0.30
29[a]	π (C1−C2)/1.93	n_1 (C2,C2′)[c]/1.75	n_2 (C2,C2′)[d]/0.37
30[a]	π (C1−C1′)/1.84	n_{sp} (C2)/1.92	p (C2)/0.28
33[a]	π (C1−C2)/1.93	n_1 (C2,C2′)[c]/1.76	n_2 (C2,C2′)[d]/0.46
34[a]	π (C1−C1′)/1.88	n_{sp} (C2)/1.86	π (N3−C2)/1.97
36[b]	π (C1−C2)/1.94	n_1 (C2,C2′)[c]/1.72	n_2 (C2,C2′)[d]/0.39
37[b]	π (C1−C1′)/1.81	n_{sp} (C2)/1.93	π (O3−C2)/1.97

[a]HF/aug-cc-pvdz//B2PLYPD/aug-cc-pVDZ. [b]HF/6-311++G**//B2PLYPD/6-31+G**. [c]n_1 antibonding linear combination (b_u) of the nonbonding orbitals at C2 and C2′. [d]n_2 bonding linear combination (a_g) of the nonbonding orbitals at C2 and C2′.

are found as possible products. These species are stabilized by the electron-donating effects of the adjacent oxygen and nitrogen atoms. In the case of the nitrogen-containing compounds, the 1,4-dicarbens are much more stable than the corresponding 1,4-biradicals, whereas in the case of the oxygen-containing compounds, 1,4-biradicals and 1,4-dicarbenes show similar energies.

At first glimpse, the products **30**, **34**, and **37** seem rather far-fetched. However, if one realizes that they are novel members of the nucleophilic carbene family,[20] a broad interest is warranted. The above-mentioned dicarbenes should yield unknown Fischer-carbenes (**39**) with reactive transition metal carbonyls, such as **38** (see Scheme 7).[21]

Scheme 7. Reaction of Carbonyl Complexes 38a and 38b with 37 To Yield the Fischer−Carbene Complexes 39a and 39b

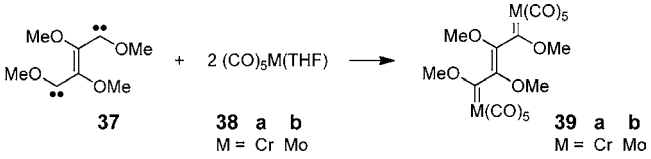

37 **38 a b** M = Cr Mo **39 a b** M = Cr Mo

Similar reactions are expected with $CpMn(CO)_2(THF)$[22] and **37**. The further use of such Fischer-carbenes in chemistry has been described in textbooks on organotransition metal chemistry.[23] The isolation of Ag(I), Au(I), and Pd(II) complexes of *N*-heterocyclic carbenes and their application in catalysis[24,25] opens also new perspectives for the nucleophilic dicarbenes of type **37**. In Scheme 8, we have depicted three possible structures for Ag(I), Au(I), and Pd(II) complexes (**40a**, **40b**, and **41**) with **37**.

Scheme 8. Possible Structures for Ag(I), Au(I), and Pd(II) Complexes Obtained from 37

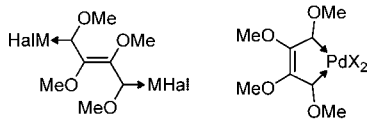

40 a b M = Ag Au **41**

The systems sketched in Schemes 7 and 8 are not only very interesting per se but can be used to trap the dicarbenes and shift the equilibrium between biradicals and dicarbenes in favor of the dicarbenes.

The dimerization reactions of two alkyne units discussed in the last paragraph should also be relevant with respect to the stability of alkynes. Dialkoxyacetylenes and bis(dialkylamino)-acetylenes are described in the literature.[26] Dimethoxy- and diethoxyacetylenes are reported to be highly reactive and stable below −40 °C.[27] The thermal stability of dialkoxyalkynes improves when bulky groups (e.g., isopropyl or *t*-butyl) are used as substituents.[28] The bis(dialkylamino)acetylenes are reported to be more stable than the dimethoxy congeners, and several procedures for their preparation are known.[26,29] Our calculations suggest a dimerization of two substituted alkyne units such as **27**, **31**, or **35**, which will lead to 1,3-butadien-1,4-diyl intermediates or electron-rich dicarbenes. Furthermore, the calculations predict that the activation barriers of dialkoxyalkynes should be lower than those of bis(dialkylamino)-acetylenes, which is consistent with the experimental stability of these compounds. Also related to our model calculations are studies on the solid-state polymerization of 1,4-disubstituted 1,3-butadiynes (Scheme 9).[30] ESR spectroscopic and optical absorption spectroscopy at low temperatures[31] reveal biradical and dicarbene intermediates.

Scheme 9. Solid-State Polymerization of 1,3-Diynes To Yield a *trans*-Polybutadiyne

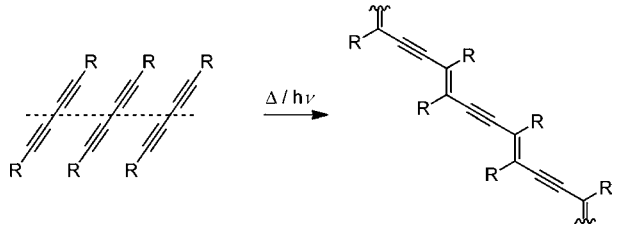

■ ASSOCIATED CONTENT

Supporting Information

Cartesian coordinates and absolute energies for all calculated compounds and complete ref 6. This material is available free of charge via the Internet at http://pubs.acs.org.

■ AUTHOR INFORMATION

Corresponding Author

gebhard.haberhauer@uni-due.de; rolf.gleiter@oci.uni-heidelberg.de

Notes

The authors declare no competing financial interest.

■ ACKNOWLEDGMENTS

This work was supported by the Deutsche Forschungsgemeinschaft (DFG). We thank Prof. Georg Jansen (Essen), Prof.

Peter Hofmann (Heidelberg), and Prof. Doris Kunz (Tübingen) for helpful discussions.

REFERENCES

(1) Mitchell, R. H.; Sondheimer, F. *Tetrahedron* **1970**, *26*, 2141−2150.
(2) Staab, H. A.; Ipaktschi, J.; Nissen, A. *Chem. Ber.* **1971**, *104*, 1182−1190.
(3) Myers, A. G.; Finney, N. S. *J. Am. Chem. Soc.* **1992**, *114*, 10986−10987.
(4) (a) Gleiter, R.; Ritter, J. *Angew. Chem., Int. Ed. Engl.* **1994**, *33*, 2470−2472. (b) Weigl, H.; Gleiter, R. *Tetrahedron Lett.* **1997**, *38*, 1541−1542. (c) Gleiter, R.; Weigl, H.; Haberhauer, G. *Eur. J. Org. Chem.* **1998**, 1447−1453.
(5) (a) Roth, W. R.; Wasser, T.; Gleiter, R.; Weigl, H. *Liebigs Ann./Recueil* **1997**, 1329−1331. (b) Haberhauer, G.; Gleiter, R. *J. Am. Chem. Soc.* **1999**, *121*, 4664−4668.
(6) Pople, J. A.; et al. *Gaussian 09*, revision A.02; Gaussian, Inc.: Wallingford, CT, 2009.
(7) Werner, H.-J.; Knowles, P. J.; Knizia, G.; Manby, F. R.; Schütz, M.; et al. *MOLPRO, version 2012.1, a package of ab initio programs*; see http://www.molpro.net.
(8) (a) Grimme, S. *J. Chem. Phys.* **2006**, *124*, 034108. (b) Schwabe, T.; Grimme, S. *Phys. Chem. Chem. Phys.* **2007**, *9*, 3397.
(9) (a) Bartlett, R. J.; Purvis, G. D., III. *Int. J. Quantum Chem.* **1978**, *14*, 561−581. (b) Pople, J. A.; Head-Gordon, M.; Raghavachari, K. *J. Chem. Phys.* **1987**, *87*, 5968−5975.
(10) Raghavachari, K.; Pople, J. A. *Int. J. Quantum Chem.* **1978**, *14*, 91−100.
(11) Møller, C.; Plesset, M. S. *Phys. Rev.* **1934**, *46*, 618−622.
(12) (a) Werner, H.-J.; Knowles, P. J. *J. Chem. Phys.* **1985**, *82*, 5053−5063. (b) Knowles, P. J.; Werner, H.-J. *Chem. Phys. Lett.* **1985**, *115*, 259−267.
(13) Celani, P.; Werner, H.-J. *J. Chem. Phys.* **2000**, *112*, 5546−5557.
(14) (a) Ditchfield, R.; Hehre, W. J.; Pople, J. A. *J. Chem. Phys.* **1971**, *54*, 724. (b) Hehre, W. J.; Ditchfield, R.; Pople, J. A. *J. Chem. Phys.* **1972**, *56*, 2257. (c) Hariharan, P. C.; Pople, J. A. *Theor. Chem. Acc.* **1973**, *28*, 213−222.
(15) (a) Dunning, T. H., Jr. *J. Chem. Phys.* **1989**, *90*, 1007−1023. (b) Kendall, R. A.; Dunning, T. H., Jr.; Harrison, J. *J. Chem. Phys.* **1992**, *96*, 6796−6806. (c) Peterson, K. A.; Woon, D. E.; Dunning, T. H., Jr. *J. Chem. Phys.* **1994**, *100*, 7410−7415. (d) Wilson, A. K.; van Mourik, T.; Dunning, T. H., Jr. *J. Mol. Struct. (THEOCHEM)* **1996**, *388*, 339−349.
(16) (a) McLean, A. D.; Chandler, G. S. *J. Chem. Phys.* **1980**, *72*, 5639−5648. (b) Raghavachari, K.; Binkley, J. S.; Seeger, R.; Pople, J. A. *J. Chem. Phys.* **1980**, *72*, 650−654.
(17) (a) Bergman, R. G. *Acc. Chem. Res.* **1973**, *6*, 25−31. (b) Jones, R. R.; Bergman, R. G. *J. Am. Chem. Soc.* **1972**, *94*, 660−661. (c) Lockhart, T. P.; Bergman, R. G. *J. Am. Chem. Soc.* **1981**, *103*, 4091−4096. (d) Lockhart, T. P.; Comita, P. B.; Bergman, R. G. *J. Am. Chem. Soc.* **1981**, *103*, 4082−4090. (e) Lindh, R.; Persson, B. J. *J. Am. Chem. Soc.* **1994**, *116*, 4963−4969. (f) Lindh, R.; Lee, T. J.; Bernhardsson, A.; Persson, B. J.; Karlström, G. *J. Am. Chem. Soc.* **1995**, *117*, 7186−7194. (g) Kraka, E.; Cremer, D. *J. Am. Chem. Soc.* **1994**, *116*, 4929−4936.
(18) (a) Hoffmann, R.; Imamura, A.; Hehre, W. J. *J. Am. Chem. Soc.* **1968**, *90*, 99−1509. (b) Hoffmann, R. *Acc. Chem. Res.* **1971**, *4*, 1−9. (c) Most recent review: Gleiter, R.; Haberhauer, G. *Aromaticity and Other Conjugation Effects*; Wiley-VCH: Weinheim, 2012; pp 217−282.
(19) Reed, A. E.; Curtiss, L. A.; Weinhold, F. *Chem. Rev.* **1988**, *88*, 899−926.
(20) (a) Bourissou, D.; Guerret, O.; Gabbaï, F. P.; Bertrand, G. *Chem. Rev.* **2000**, *100*, 39−91. (b) De Frémont, P.; Marion, N.; Nolan, S. P. *Coord. Chem. Rev.* **2009**, *253*, 862−892.
(21) Raubenheimer, H. G.; Swanepoel, H. E. *J. Organomet. Chem.* **1977**, *141*, C21−C22.
(22) (a) Herrmann, W. A. *Angew. Chem., Int. Ed. Engl.* **1974**, *13*, 599. (b) Herrmann, W. A.; Plank, J.; Ziegler, M. L.; Weidenhammer, K. *Angew. Chem., Int. Ed. Engl.* **1978**, *17*, 777.
(23) Collman, J. P.; Hegedus, L. S.; Norton, J. R.; Finke, R. G. *Principles and Applications of Organotransition Metal Chemistry*; University Science Books: Mill Valley, CA, 1987.
(24) Schneider, S. K.; Herrmann, W. A.; Herdtweck, E. *Z. Anorg. Allg. Chem.* **2003**, *629*, 2363−2370.
(25) (a) Wang, H. M. J.; Lin, I. J. B. *Organometallics* **1998**, *17*, 972−975. (b) Wang, H. M. J.; Chen, C. Y. L.; Lin, I. J. B. *Organometallics* **1999**, *18*, 1216−1223. (c) Herrmann, W. A.; Elison, M.; Fischer, J.; Köcher, C.; Artus, G. R. J. *Angew. Chem., Int. Ed. Engl.* **1995**, *34*, 2371−2374.
(26) (a) Review: Gleiter, R.; Werz, D. B. *Chem. Rev.* **2010**, *110*, 4447−4488. (b) *Chemistry of Acetylenes*; Viehe, H. G., Ed.; Marcel Dekker: New York, 1969. (c) Witulski, B.; Alayrac, C. *Science of Synthesis*; Thieme: Stuttgart, 2006; Vol. *24.3*, pp 821−833.
(27) Messeguer, A.; Serratosa, F.; Rivera, J. *Tetrahedron Lett.* **1973**, *14*, 2895−2898.
(28) (a) Pericás, M. A.; Serratosa, F. *Tetrahedron Lett.* **1977**, *18*, 4433−4436. (b) Bou, A.; Pericás, M. A.; Serratosa, F. *Tetrahedron* **1981**, *37*, 1441−1449.
(29) Réne, L.; Janousek, Z.; Viehe, H. G. *Synthesis* **1982**, 645.
(30) (a) Wegner, G. *Z. Naturforsch.* **1969**, *24b*, 824−832. (b) Wegner, G. *Makromol. Chem.* **1972**, *154*, 35−48.
(31) (a) Review: Sixl, H. *Adv. Polym. Sci.* **1984**, *63*, 49−90. (b) Huber, R. A.; Schwoerer, M.; Benk, H.; Sixl, H. *Chem. Phys. Lett.* **1981**, *78*, 416−420.